2003

Toward Aerosol/Cloud Condensation Nuclei (CCN) Closure During CRYSTAL-FACE

VanReken, Timothy M.

Toward aerosol/cloud condensation nuclei (CCN) closure during CRYSTAL-FACE

Timothy M. VanReken,[1] Tracey A. Rissman,[1] Gregory C. Roberts,[2]
Varuntida Varutbangkul,[1] Haflidi H. Jonsson,[3] Richard C. Flagan,[1] and John H. Seinfeld[1]

Received 10 March 2003; revised 1 July 2003; accepted 15 July 2003; published 18 October 2003.

[1] During July 2002, measurements of cloud condensation nuclei were made in the vicinity of southwest Florida as part of the Cirrus Regional Study of Tropical Anvils and Cirrus Layers-Florida Area Cirrus Experiment (CRYSTAL-FACE) field campaign. These observations, at supersaturations of 0.2 and 0.85%, are presented here. The performance of each of the two CCN counters was validated through laboratory calibration and an in situ intercomparison. The measurements indicate that the aerosol sampled during the campaign was predominantly marine in character: the median concentrations were 233 cm^{-3} (at $S = 0.2\%$) and 371 cm^{-3} (at $S = 0.85\%$). Three flights during the experiment differed from this general trend; the aerosol sampled during the two flights on 18 July was more continental in character, and the observations on 28 July indicate high spatial variability and periods of very high aerosol concentrations. This study also includes a simplified aerosol/CCN closure analysis. Aerosol size distributions were measured simultaneously with the CCN observations, and these data are used to predict a CCN concentration using Köhler theory. For the purpose of this analysis, an idealized composition of pure ammonium sulfate was assumed. The analysis indicates that in this case, there was good general agreement between the predicted and observed CCN concentrations: at $S = 0.2\%$, $N_{predicted}/N_{observed} = 1.047$ ($R^2 = 0.911$); at $S = 0.85\%$, $N_{predicted}/N_{observed} = 1.201$ ($R^2 = 0.835$). The impacts of the compositional assumption and of including in-cloud data in the analysis are addressed. The effect of removing the data from the 28 July flight is also examined; doing so improves the result of the closure analysis at $S = 0.85\%$. When omitting that atypical flight, $N_{predicted}/N_{observed} = 1.085$ ($R^2 = 0.770$) at $S = 0.85\%$. *INDEX TERMS:* 0305 Atmospheric Composition and Structure: Aerosols and particles (0345, 4801); 0320 Atmospheric Composition and Structure: Cloud physics and chemistry; 1610 Global Change: Atmosphere (0315, 0325); *KEYWORDS:* CCN closure, CCN instrumentation, CRYSTAL-FACE, aircraft measurements, cloud

Citation: VanReken, T. M., T. A. Rissman, G. C. Roberts, V. Varutbangkul, H. H. Jonsson, R. C. Flagan, and J. H. Seinfeld, Toward aerosol/cloud condensation nuclei (CCN) closure during CRYSTAL-FACE, *J. Geophys. Res.*, *108*(D20), 4633, doi:10.1029/2003JD003582, 2003.

1. Introduction

[2] The importance of clouds in the climate system is well established; clouds play a vital role in the global radiation budget and hydrological cycle. Clouds form when a parcel of air becomes supersaturated with respect to water vapor and the excess water condenses rapidly on ambient particles to form droplets. For this rapid condensation (termed activation) to occur at a given supersaturation, the particle must have sufficient soluble mass; this subset of the aerosol population is called cloud condensation nuclei, denoted CCN. The atmospheric concentration of CCN is often substantially enhanced by human activities, and the various ways that this enhancement affects the radiative properties of clouds are collectively known as indirect aerosol forcing (the inclusion of the word ''indirect'' differentiates these effects from the direct aerosol effect, which describes the radiative interactions of the particles themselves). Cloud processes are complex by nature and heavily dependent on purely dynamical factors, but in general terms indirect aerosol effects can be split into two categories. For a given supersaturation, an air mass with a higher CCN concentration would produce a cloud with a higher droplet concentration, but a smaller mean droplet diameter; this often results in a more reflective cloud and is known as the first indirect effect or Twomey effect [*Twomey*, 1977]. The second indirect effect, identified by *Albrecht* [1989], also stems from the smaller average droplet diameter in polluted clouds; a smaller mean droplet size inhibits the processes

[1]Department of Chemical Engineering, California Institute of Technology, Pasadena, California, USA.
[2]Center for Atmospheric Sciences, Scripps Institution of Oceanography, San Diego, California, USA.
[3]Center for Interdisciplinary Remotely Piloted Aircraft Studies, United States Naval Postgraduate School, Marina, California, USA.

0148-0227/03/2003JD003582

that lead to precipitation, thereby increasing cloud lifetime and therefore cloud coverage.

[3] While observations support the existence of indirect aerosol effects on a local scale [*Johnson et al.*, 1996; *Rosenfeld*, 1999, 2000; *Durkee et al.*, 2000; *Garrett et al.*, 2002], current understanding of the processes involved is insufficient to accurately predict the global importance of indirect aerosol forcing. The *Intergovernmental Panel on Climate Change* (*IPCC*) [2001] estimates that the first indirect effect results in a global mean forcing of between 0 and -2 W m^{-2} and does not give an estimate for the second indirect effect, which is also expected to be one of cooling. Reliable predictions regarding climate forcing await more detailed understanding of the dependence of cloud properties on aerosol properties.

[4] The first step in understanding the relationship between the ambient aerosol and the cloud that forms therefrom is to know the activation properties of the atmospheric aerosol. In theory, if a particle's size and chemical composition were precisely known, the supersaturation at which activation occurs could be calculated using Köhler theory [*Seinfeld and Pandis*, 1998]. However, ambient aerosol populations can contain myriad chemical species, the activation properties of most of which have not been established. Furthermore, recent studies have demonstrated that simply categorizing aerosol species into soluble and insoluble fractions is sometimes insufficient [*Cruz and Pandis*, 1998; *Hegg et al.*, 2001; *Raymond and Pandis*, 2002]; slightly soluble species, surfactants, and soluble gases can affect activation either thermodynamically or kinetically [*Charlson et al.*, 2001; *Nenes et al.*, 2002]. To establish the connection between theory and the actual atmosphere, it is desirable to directly measure the portion of the aerosol population that activates at a given supersaturation. Such a measurement generally involves exposing an aerosol sample to a known supersaturation; the CCN active at that supersaturation rapidly grow to a size at which they can be counted by standard techniques. In the laboratory, instruments using such measurement strategies can be tested using aerosols whose size and chemical properties are carefully controlled. Then, the activation behavior of an ambient aerosol can be measured, giving rise to a so-called closure experiment, whereby measured CCN concentrations are compared against predictions based on simultaneously measured aerosol size and composition data. A successful closure study serves to validate both the performance of the CCN instrument itself and the theoretical basis for the prediction of the activation properties of the aerosol.

[5] The Cirrus Regional Study of Tropical Anvils and Cirrus Layers-Florida Area Cirrus Experiment (CRYSTAL-FACE) field campaign in the Florida Keys during July 2002 had as its goal the investigation of the properties of tropical convective systems and the resultant cirrus layers. These cirrus layers, known as anvils, affect the radiative balance [*Ramanathan et al.*, 1989], and a detailed understanding of the physical processes involved in their formation would enhance the ability to predict their occurrence and lifetime. As part of the CRYSTAL-FACE campaign, the Center for Interdisciplinary Remotely Piloted Aircraft Studies (CIRPAS) Twin Otter aircraft flew 20 research missions, focused on characterizing the ambient aerosol in the vicinity of the convective systems, measuring cloud properties, and on making radiation measurements below the cirrus anvils. Data were collected both over land and water along the southwest coast of Florida; Figure 1 shows the flight tracks for the missions for which CCN data are available. Table 1 provides details on each research flight, and Table 2 lists the aerosol and gas-phase instrumentation on board the Twin Otter.

[6] This study presents the airborne CCN measurements from CRYSTAL-FACE and examines the extent to which it is possible to predict CCN concentrations from size distribution data in the absence of a detailed knowledge of the aerosol composition. Two CCN counters were on board the Twin Otter (Table 2). One instrument, operating at a supersaturation of approximately 0.85%, provided useful data for all but three flights, when electrical noise from another instrument caused the CCN counter to malfunction. The second CCN counter, with an effective supersaturation of approximately 0.2%, was operated for all but one flight from CF-8 through the end of the campaign; no data are available from CF-16 due to an instrument malfunction. The reliability of these measurements is verified by laboratory experiments, by a field intercomparison of the two instruments, and by comparison with other instruments measuring aerosol concentration. After establishing the validity of the data, the observations are described in more detail in order to provide a comprehensive picture of the typical summertime CCN population over southwest Florida. A simplified closure analysis follows, comparing the CCN data set at both measured supersaturations to size spectral data from the Caltech differential mobility analyzer (DMA, described by *Wang et al.* [2003]), assuming an idealized (ammonium sulfate) composition. The study concludes by discussing the sensitivity of the results to assumptions made in the analysis.

2. Background

[7] Previous attempts to match predicted CCN concentrations with those directly observed have met with mixed success. The methods by which these studies were conducted vary considerably, and by examining the details of these methodologies one can determine those elements required for a successful experiment.

[8] Only three studies in the literature present results that can be considered successful in terms of aerosol/CCN closure. All were ground-based studies: *Liu et al.* [1996] made measurements in Nova Scotia as part of the North Atlantic Regional Experiment (NARE), *Cantrell et al.* [2001] used measurements made in the Maldives during the Indian Ocean Experiment (INDOEX), and *Roberts et al.* [2002] collected data in the Amazon Basin during the Cooperative Large-Scale Biosphere-Atmosphere (LBA) Airborne Regional Experiment 1998 (CLAIRE-98). In the first two studies, the aerosol was split into soluble and insoluble fractions based on filter samples and the soluble fraction was assumed to be ammonium sulfate. Roberts et al. further split the soluble fraction into organic and inorganic components. All three studies averaged the CCN and size spectral data over a substantial period of time to match the filter sampling time. Liu et al. used an isothermal haze chamber to obtain CCN concentrations at a supersaturation,

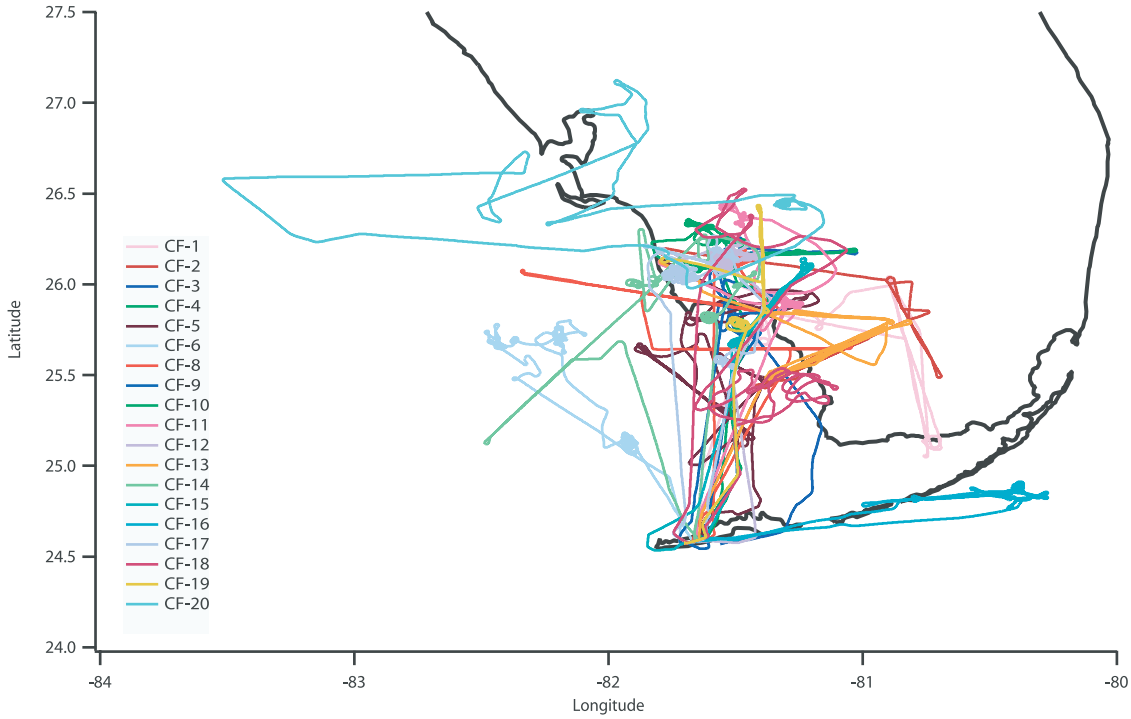

Figure 1. Flight tracks for the CRYSTAL-FACE flights for which CCN data are available.

$S = 0.06\%$; these data were compared against integrated size distributions from an optical particle counter (Particle Measurement Systems model PCASP-100X). For each of the 12 samples in the closure analysis, data were averaged for a period of 2–5 hours. In 10 of the 12 sampling intervals, the predicted concentration agreed with the measurement within the uncertainty limits; of the other two samples, in one case the measurement was overpredicted, and in one case it was underpredicted. Cantrell et al. measured CCN spectra for supersaturations between 0.1 and 1% using the CCN Remover described by *Ji et al.* [1998]; in this case, the aerosol-size distribution was measured using a scanning mobility particle sizer (SMPS) (TSI, Inc.). The average measured spectra from three dates were compared to predicted concentrations based on the filter cut sizes. Eight of the 10 data points matched within experimental uncertainties; in the other two cases, the predicted CCN spectra exceeded the measurements. In the Roberts et al. study, CCN measurements were made at several supersaturations using a static thermal-gradient chamber. These data were averaged over 48–72 hour periods to match the sampling time for the microorifice uniform deposit impactor (MOUDI) cascade impactors that were the source of the compositional data in the analysis. As in the Cantrell et al. study, aerosol-size spectra were measured with a differential mobility analyzer. For each of the four sampling periods, the calculated CCN spectrum agreed with the observation to within measurement uncertainties. Although these studies were limited in scope, the measured and predicted CCN concentrations agreed well enough to indicate that closure had been achieved.

[9] Other ground-based studies of CCN closure have been less successful. A common characteristic is that measured CCN concentrations were less than would be predicted based on available size and composition information. In measurements carried out at Cape Grim, Australia, *Bigg* [1986] used measured size distributions and assumed that the aerosol was composed of either sodium chloride or ammonium sulfate; this produced reasonable results at low CCN concentrations, but there were large discrepancies at higher CCN concentrations. Studies by *Covert et al.* [1998] and *Zhou et al.* [2001] (a ship-based study) each compared two methods for predicting CCN concentrations. Both studies used data from tandem differential mobility analyzers to infer an insoluble fraction using hygroscopic growth information and assumed that the soluble fraction was ammonium sulfate. In the Covert

Table 1. Summary of Twin Otter Missions for the CRYSTAL-FACE Campaign

Flight Number	Date	Launch Time, UT	Flight Duration, hours	Mission Type	CCN Data 0.2%	CCN Data 0.85%
CF-1	3 July	1159	4.01	radiation	no	yes
CF-2	3 July	1750	3.03	radiation	no	yes
CF-3	6 July	1234	3.13	radiation	no	yes
CF-4	7 July	1223	3.14	cloud	no	yes
CF-5	7 July	1723	4.44	radiation	no	yes
CF-6	10 July	1404	3.41	cloud	no	yes
CF-7	11 July	1525	4.44	radiation	no	no
CF-8	13 July	1725	4.54	cloud, radiation	yes	no
CF-9	16 July	1752	2.16	clear air	yes	no
CF-10	18 July	1424	2.30	cloud	yes	yes
CF-11	18 July	1800	2.59	radiation	yes	yes
CF-12	19 July	1458	2.50	cloud	yes	yes
CF-13	19 July	1901	4.06	radiation	yes	yes
CF-14	21 July	1713	4.21	radiation	yes	yes
CF-15	23 July	1929	4.24	radiation	yes	yes
CF-16	25 July	1400	2.09	cloud	no	yes
CF-17	26 July	1556	4.03	cloud	yes	yes
CF-18	28 July	1831	4.03	radiation	yes	yes
CF-19	29 July	1328	1.27	clear air	yes	yes
CF-20	29 July	1700	4.10	radiation	yes	yes

Table 2. Twin Otter Aerosol and Trace Gas Payload During CRYSTAL-FACE

Instrument	Measurement	Sampling Interval, s
Aerosol mass spectrometer (AMS)	particle size and composition: 50 nm to 1.0 μm	60
Aerodynamic Particle Sizer (APS)	size distribution: 0.37–2.0 μm	27
Carbon monoxide (CO)	carbon monoxide concentration	1
Cloud condensation nucleus counter (Caltech)	CCN at S_c = 0.85%	2
Cloud condensation nucleus counter (Scripps)	CCN at S_c = 0.2%	1
Condensation particle counters (CPCs)	particle concentration: cut sizes at 3, 7, and 12 nm	1
Differential mobility analyzer (DMA)	aerosol size distribution: 10–900 nm	103
Multisample aerosol collection system (MACS)	aerosol samples for transmission electron microscopy (TEM) analysis	variable (min)
Water Vapor (NOAA)	water vapor concentration	1
Cloud, Aerosol, Precipitation Spectrometer (CAPS)	size distribution: 0.3 μm to 1.6 mm	1
Forward Scattering Spectrometer Probe (FSSP-100)	size distribution: 0.5–47 μm	1
Passive cavity aerosol spectrometer probe (PCASP)	size distribution: 0.1–3.0 μm	1
Microorifice uniform deposit impactor (MOUDI)	size-classified filter sampling	variable (hours)

et al. study, the correlation between measured and predicted CCN improved when particle solubility was taken into account. Zhou et al., following the same procedure, did not see an improved correlation, and concluded that this was due to a very low insoluble fraction. In both cases, the measured CCN concentration was, on average, 20–30% lower than that predicted; while this error is, perhaps, not excessive, a consistent overprediction is indicative of either a problem with the measurement or an incomplete understanding of the processes affecting activation.

[10] Airborne closure studies are inherently more difficult than those that are ground-based, and the results of the few available airborne closure studies reflect this difficulty. A moving platform greatly increases the variability in the aerosol population sampled, making rapid measurements necessary. Space considerations on the aircraft often limit the instrumentation available; the resulting sacrifices in the data set add further uncertainty to an already demanding measurement. In short, aerosol/CCN closure has not yet been demonstrated from an airborne platform. An attempt by *Martin et al.* [1994] consisted of only two data points, one maritime and one polluted. The authors assumed a pure ammonium sulfate aerosol and compared the CCN measurement with an integrated spectrum from an optical particle counter. There was reasonable agreement in the maritime case but not in the polluted case. In the second Aerosol Characterization Experiment (ACE-2), *Snider and Brenguier* [2000], using data from the Météo-France Merlin aircraft, compared measured CCN with size spectra from a optical particle sizing instrument (passive cavity aerosol spectrometer probe (PCASP)), assuming a pure ammonium sulfate composition. The measured CCN concentration (at S = 0.2%) was roughly half that expected from the PCASP data; the difference was attributed to an incomplete understanding of the aerosol composition. *Wood et al.* [2000] undertook a similar analysis during ACE-2, using data from the UK Meteorological Office C-130 aircraft, and attempted to improve the agreement by varying the assumed soluble aerosol fraction. At high supersaturations (S > 0.5%), the CCN concentrations were overpredicted by more than 50%; no explanation was offered for this disagreement. Also, during ACE-2, *Chuang et al.* [2000a] measured CCN at $S \approx$ 0.1% from the CIRPAS Pelican and predicted CCN concentrations based on airborne size distributions and aerosol composition measurements from ground-based filter samples. Measurements were roughly an order of magnitude lower than predictions; the authors surmised that instrumentation problems were the source of most of the discrepancy.

[11] In summary, in most of the published closure studies, measured CCN concentrations are significantly lower than expected based on theoretical activation of the measured aerosol-size distributions. This disagreement has usually been attributed to an incomplete understanding of the activation processes, even when sampling relatively clean air masses. However, in three cases, closure was generally achieved despite the use of a relatively simple compositional model: *Liu et al.* [1996], *Cantrell et al.* [2001], and *Roberts et al.* [2002]. While in some cases a lack of closure may be due to measurement errors, this still leaves open the basic question of whether it is possible to achieve an aerosol/CCN closure.

3. CCN Instrument Descriptions

[12] Both CCN counters deployed during CRYSTAL-FACE are based on the instrument described by *Chuang et al.* [2000b], using an improved temperature configuration first identified by *Rogers and Squires* [1981] and brought to fruition by G. C. Roberts and A. Nenes (manuscript in preparation, 2003, hereinafter referred to as Roberts and Nenes, manuscript in preparation, 2003). The instrument described by *Chuang et al.* [2000b] was intended to function as a CCN spectrometer, where the supersaturation at which particles activated could be inferred from the droplet diameter at the outlet. However, during the ACE-2 campaign, in which that instrument flew aboard the CIRPAS Pelican, stability and resolution issues limited its usefulness, and data were reported only for a single supersaturation [*Chuang et al.*, 2000a]. Later work also discussed by *Chuang et al.* [2000b] indicated that those resolution issues were characteristic of the temperature configuration employed during ACE-2, a result that was later verified theoretically by *Nenes et al.* [2001].

[13] Recent work by Roberts and Nenes (manuscript in preparation, 2003) indicates that the cylindrical CCN design could be significantly improved by incorporating a different control strategy, where the temperature of the column wall is increased axially to asymptotically approach a constant supersaturation. Because water vapor diffuses more rapidly than heat, the constant streamwise temperature gradient leads to a nearly constant supersaturation on the instrument centerline. The simulated supersaturation profile arising

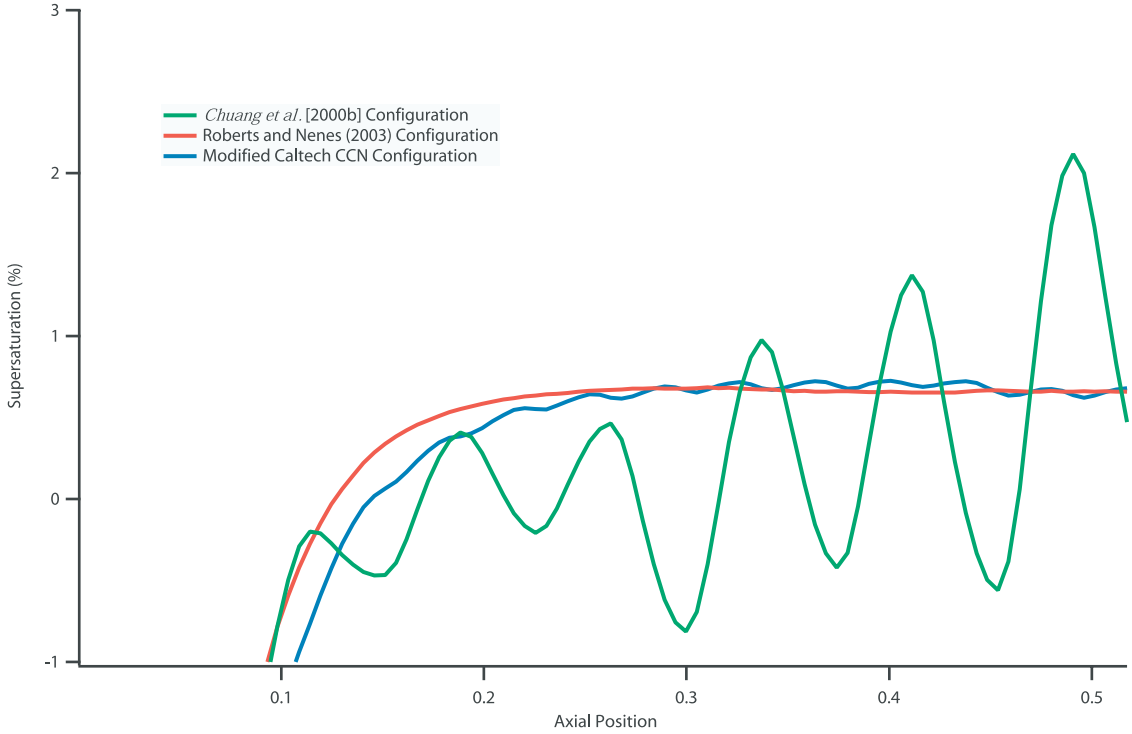

Figure 2. Simulated saturation profiles for various configurations for cylindrical CCN instruments. Both the Roberts and Nenes (manuscript in preparation, 2003) configuration and the current configuration of the Caltech instrument are substantial improvements over the design described by *Chuang et al.* [2000b].

from this new temperature configuration is compared to that of the *Chuang et al.* [2000b] configuration in Figure 2. The constant temperature increase clearly creates a more stable saturation profile. The new configuration also significantly simplifies the instrument, since ideally it requires active temperature control only at the beginning and end of the growth chamber, compared to the numerous independently controlled segments in the original configuration.

[14] For the CRYSTAL-FACE campaign, both the instrument described by Roberts and Nenes (manuscript in preparation, 2003) (the Scripps CCN counter) and the Caltech CCN counter were on board the Twin Otter. The Caltech counter, described by *Chuang et al.* [2000b], was modified to incorporate a variation on the improved temperature profile developed by Roberts and Nenes (manuscript in preparation, 2003). Instead of controlling actively only at the top and bottom of the growth chamber, 14 independent sections are maintained, with a constant temperature increase in each section. The temperatures in the first and last sections are controlled with thermoelectric coolers, and resistive heaters are used to maintain the temperature in the intermediate sections (see Figure 3). Using the model described by *Nenes et al.* [2001], the saturation profile for this configuration was simulated and is presented along with the others in Figure 2; the result is close to that of the idealized linear profile. The Caltech instrument was originally designed for stepwise variation in the wall temperature, leading to the slight oscillations in the temperature profile when operated in this mode.

[15] Other technical improvements were made to the Caltech CCN Counter prior to its use in the CRYSTAL-

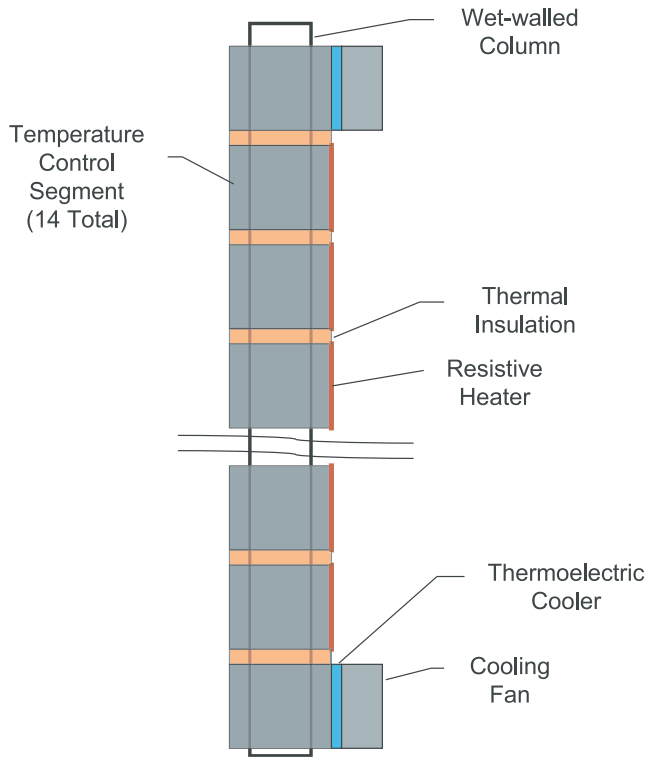

Figure 3. Schematic of the Caltech CCN counter as configured during CRYSTAL-FACE.

FACE campaign (see *Chuang et al.* [2000b] for details on the original instrument configuration). The sheath flow is controlled on a volumetric rather than on a mass basis, using volumetric flow controllers from Alicat Scientific Instruments. The humidification of the sheath air is now accomplished using Nafion humidifiers from Perma-Pure, Inc. The computer has been upgraded and data acquisition is managed with National Instruments LabView software; a separate multichannel analyzer card is no longer used since only the number of activated particles must be determined. The thermoelectric coolers are now driven with Wavelength Electronics MPT-5000 temperature controllers, while the resistive heaters are still driven by RHM-4000 units. Controlled resistive heaters have been added to the sheath and sample inlets and to the optical particle counter to prevent instantaneous supersaturations at the inlet and water condensation at the outlet. Finally, the wetted filter paper on the internal walls of the growth column is periodically resaturated using a peristaltic pump; while this made the instrument unavailable for data collection approximately 5% of the time, it prevented the more serious flooding and drying problems experienced in the past. These technical improvements all contributed to substantial gains in instrument stability and reliability.

4. Instrument Verification

4.1. Scripps CCN Counter

[16] The principle of the Scripps CCN instrument has been validated in controlled laboratory experiments using aerosol with known activation properties. (A detailed description of the calibration and results is presented by Roberts and Nenes (manuscript in preparation, 2003).) Monodisperse aerosol of a known composition (i.e., ammonium sulfate) and size was generated by a DMA (TSI Model 3081). Particle diameters between 0.01 and 0.6 μm were chosen to observe various degrees of activation at a particular supersaturation. The aerosol at a selected size was simultaneously sampled at the outlet of the DMA by an SMPS (TSI Model 3081), a condensation particle counter (CPC) (TSI Model 3010), and the CCN instrument. The SMPS verified the monodisperse output of the first DMA and quantified the amount of multiply charged particles. The scans were averaged, and the median diameter of the distribution was used as the calibration size for the CCN counter. The integrated droplet distribution from the SMPS yielded the total aerosol concentration and was normalized to the average number concentrations recorded by the CPC for the same SMPS scan period. Number and droplet concentrations were recorded every second by the CPC and CCN, respectively, and ranged between 0 and 10^4 cm^{-3}. The CPC has detection efficiency near 100% for particles with diameters larger than 0.018 μm and was used as a reference for comparing the activated fraction of CCN to total aerosol concentration. The median diameter of the selected monodisperse size distribution that activated 50% of the aerosol to CCN was used to calculate the corresponding supersaturation using Köhler theory.

[17] The calibration of the instrument yielded sharp activation curves, presented by Roberts and Nenes (manuscript in preparation, 2003), and verified the novel technique of generating a supersaturation profile. At a flow rate of 500 cm^3 min^{-1} and temperature difference between the ends of the column of 5°C, a sharp rise in the activated droplet concentration occurred at a median diameter of 72 nm. Theory predicts that, for ammonium sulfate aerosol, the corresponding critical supersaturation of 72-nm diameter particles is 0.24%. These calibrations were performed at ambient pressure (ca. 1000 mbar) and need to be corrected for airborne measurements at higher altitudes. The flights during CRYSTAL-FACE occurred mostly in the boundary layer around 900 mbar, which slightly lowers the supersaturation to 0.2%.

4.2. Caltech CCN Counter

[18] To verify the effective supersaturation of the Caltech CCN instrument in its new configuration, a laboratory calibration was carried out. In this experiment, the instrument was set up in the laboratory in parallel with a CPC and either ammonium sulfate or sodium chloride particles of known size were fed simultaneously to both instruments. Laboratory pressure and temperature were approximately 980 hPa and 293 K, respectively. The activation properties of these particles were calculated using Köhler theory as it is presented by *Seinfeld and Pandis* [1998]; constant van't Hoff factors (ν = 2 for sodium chloride and ν = 3 for ammonium sulfate) were used. Polydisperse aerosol distributions of each composition were generated with a nebulizer and passed through a diffusion dryer before being classified with a cylindrical DMA. The resulting monodisperse aerosol was then sampled by both the Caltech CCN counter and a TSI 3010 CPC. The sample concentrations were kept between 800 and 1500 particles cm^{-3}, somewhat above what were commonly observed during the CRYSTAL-FACE campaign.

[19] The results of the verification experiments are given in Figures 4 and 5. Figure 4 shows the CCN ratio (measured CCN concentration/particle concentration as measured by the TSI 3010) as a function of dry particle size. For both ammonium sulfate and sodium chloride, the data indicate a sharp activation transition. Vertical lines indicate the smallest dry diameters that activate in the column for each species, as predicted by the instrument model developed by *Nenes et al.* [2001]. As expected, the size at which this transition takes place is smaller for NaCl than for $(NH_4)_2SO_4$. When the CCN ratio is plotted as a function of critical supersaturation (Figure 5), the instrument's response for each species is found to be nearly identical, with the transition occurring at approximately 0.85%. During CRYSTAL-FACE, housekeeping data from the CCN counter for level legs were frequently inserted in the instrument model to determine the effective supersaturation in the instrument during that period; the results indicate that the supersaturation over the course of the campaign was typically within 5% of the value determined by the laboratory experiments.

4.3. Field Instrument Intercomparison

[20] Making airborne aerosol measurements is inherently difficult, and it is impossible to completely mimic flight conditions in the laboratory. A well-characterized instrument in the laboratory is necessary but not sufficient for a well-characterized flight instrument. As a means of verifying the in situ performance of both CCN counters,

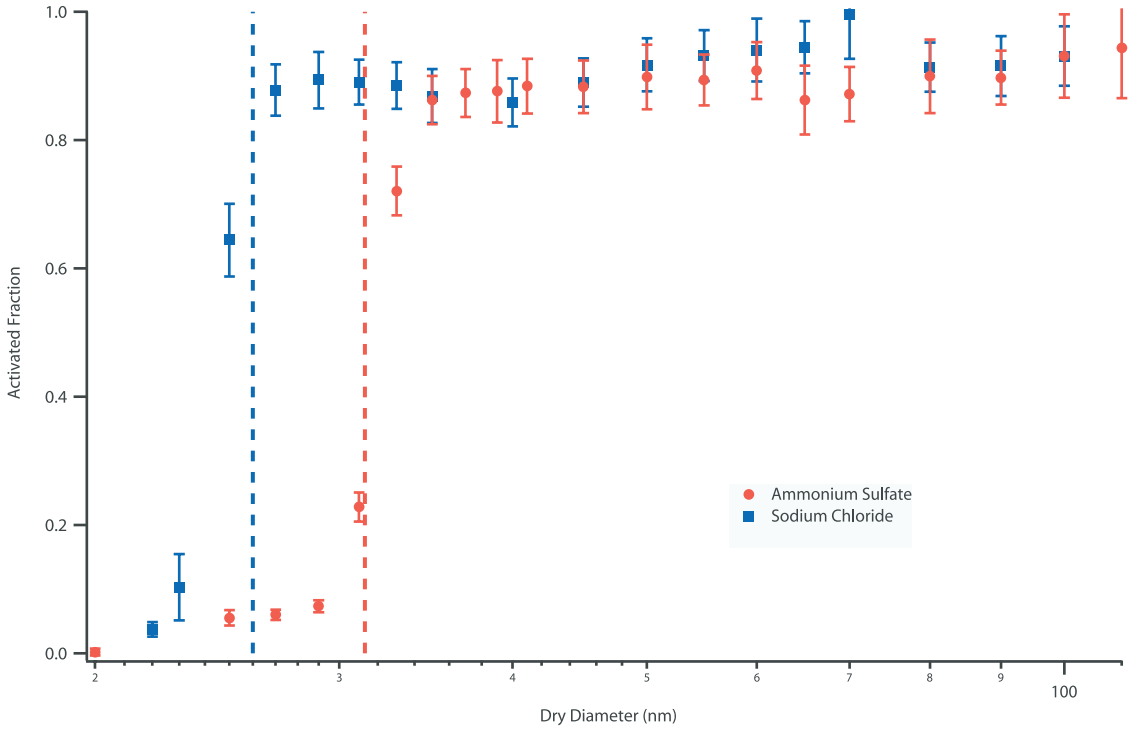

Figure 4. Activated fraction versus dry diameter from the laboratory verification experiments for the Caltech CCN instrument. The dashed lines represent the cut size predicted from the instrument model described by *Nenes et al.* [2001].

the temperature gradient of the Scripps counter was temporarily adjusted so that each had an effective supersaturation of ~0.85%. The comparison took place during CF-11, from 1914 to 1932 UTC; this time period included samples in and out of cloud and at several altitudes between 1000 and 1700 m. The time series for this period is presented in Figure 6; for easier comparison, the data from the Scripps counter are given as 2-s averages to match the slower sampling rate of the Caltech instrument. Brief gaps in the data from the Scripps instrument occur during altitude

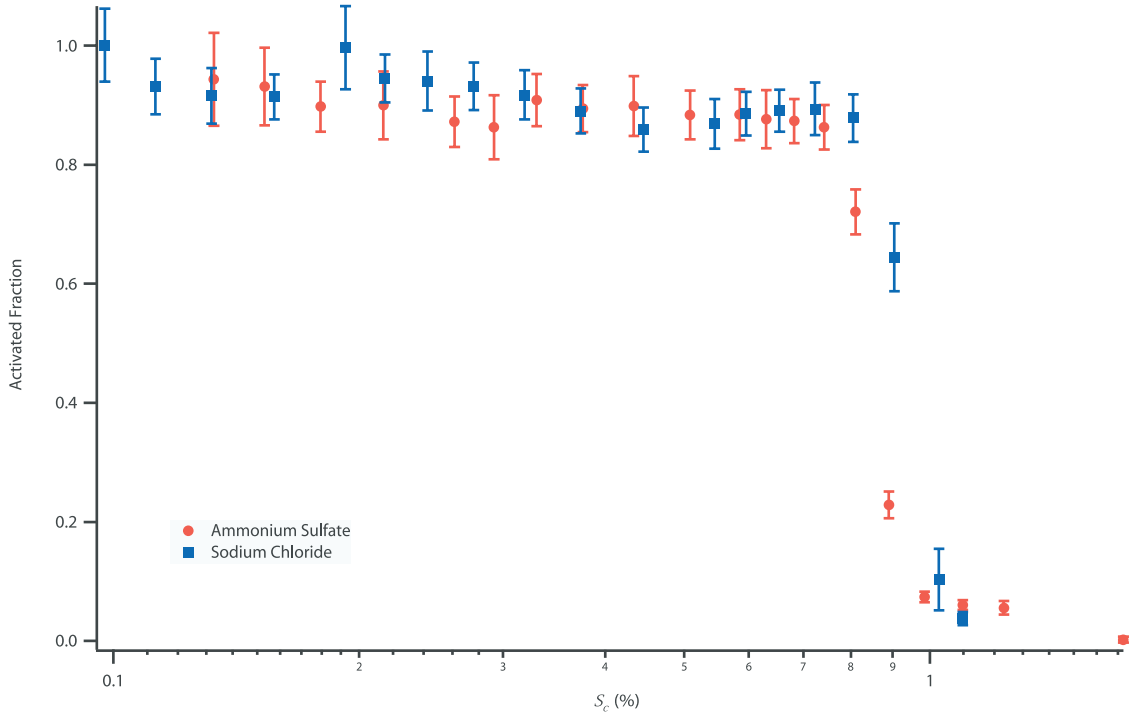

Figure 5. The data from Figure 4 plotted versus particle critical supersaturation.

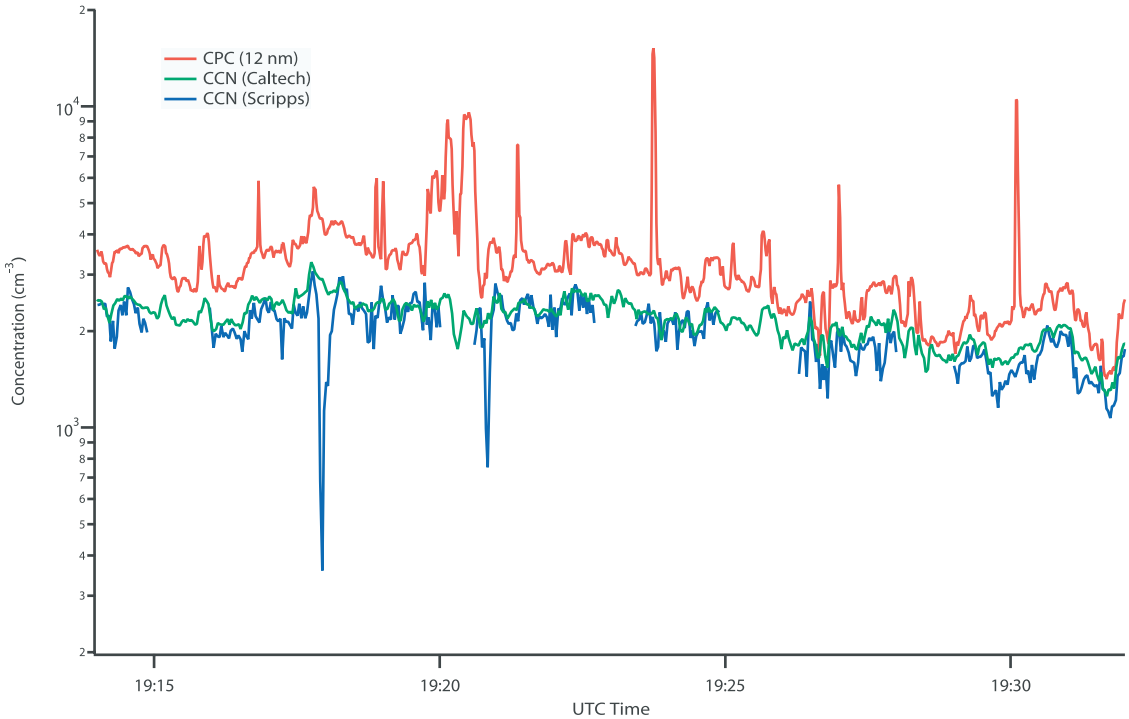

Figure 6. Time series from the in situ intercomparison of CCN instruments conducted during flight CF-11. The brief gaps in the data from the Scripps instrument occurred during altitude changes.

changes. For the purposes of the statistical comparison, these time periods are also removed from the Caltech CCN data set.

[21] The two instruments agree quite closely over the course of the comparison, except for two brief periods, each less than 20 s, where the concentration indicated by the Scripps counter decreased significantly relative to data from both instruments over the rest of the time period. Overall, agreement was excellent: the mean ratio ($N_{Scripps}/N_{Caltech}$) was 0.917, with a standard deviation of 0.115. When the two brief periods of large disagreement are omitted, the mean increases to 0.929, with a standard deviation of 0.086. In either case, the data indicate agreement between the instruments to within the standard deviation, indicating that both instruments work reliably on board the aircraft and the slightly different configurations produced similar results.

4.4. Instrument Response

[22] Another test of the validity of the CCN measurements in the field is to examine the instrument response to rapid changes in atmospheric concentrations, which can occur frequently on airborne platforms. During CRYSTAL-FACE, three TSI condensation particle counters were on board the Twin Otter and sampled from the same inlet as the CCN counters. Figure 7 displays a 30-min time series from CF-20 for one of these particle counters (operating at a nominal cut size of 12 nm), along with the corresponding data from both CCN counters. The gaps in the time series for $S = 0.2\%$ are the result of the removal of data during altitude changes. The CCN counters record several rapid changes in concentration that correspond closely with concurrent transitions in the total particle concentration measured by the CPC. For example, several sharp transitions occur between 1732 and 1735 UT that are seen clearly in the time series for all three instruments, indicating that the response times of the CCN counters to changes in the sample concentration are similar to that of the CPC. However, there are also several instances where a pulse is seen by the CPC that is not seen by one or both of the CCN counters (e.g., at 1749, 1752, and 1754 UT). This does not necessarily indicate a problem with the CCN instruments: the CPC has a smaller cut size and these pulses in the time series probably correspond to particles too small or too insoluble to activate. The time series data confirm that changes in the observed CCN concentration in situ correspond to actual changes in the aerosol population.

5. Trends in CCN During CRYSTAL-FACE

[23] Previous studies have shown that CCN concentrations, like all aerosol properties, vary substantially in space and time; therefore when comparing CCN concentrations with those of previous surface and airborne studies, the conditions of the measurements must be considered. CCN concentrations are typically lowest ($N_{CCN} < 250$ cm^{-3} for $S > 0.5\%$) under remote marine conditions in either hemisphere [*Hegg et al.*, 1991, 1995; *Hudson*, 1993; *Covert et al.*, 1998; *Cantrell et al.*, 2000]. In contrast, concentrations can be on the order of several thousand cm^{-3} where a heavy anthropogenic influence exists [*Hudson and Frisbie*, 1991; *Hitzenberger et al.*, 1999; *Cantrell et al.*, 2000].

[24] Earlier published measurements of CCN concentrations in eastern and southern Florida indicate substantial variation depending on the recent history of the air mass. *Hudson and Yum* [2001] described measurements made along the eastern coast of Florida; these data were classified based on the origin of the air mass, each flight designated either maritime or continental. Over 28,000 separate measurements were included in the analysis, with an average

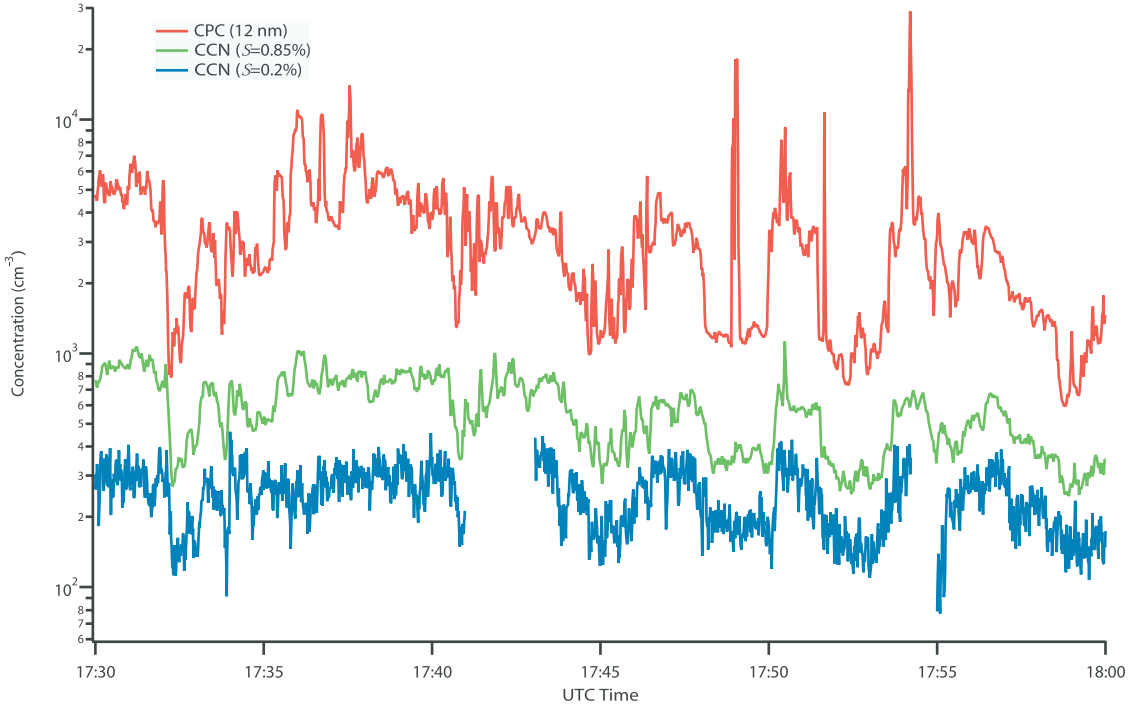

Figure 7. Time series data from flight CF-20. The altitude of the aircraft was ~1000 m until 1742 UT and ~1500 m thereafter. The gaps in the data at S = 0.2% are due to occasional instabilities in the instrument.

duration of 3.5 s. At a supersaturation of 1%, the average concentration was 359 cm^{-3} for the maritime flights and 1411 cm^{-3} for the continental flights. Concentrations were slightly lower at S = 0.85% (320 and 1300 cm^{-3}, respectively) and significantly lower at S = 0.2% (~200 and 500 cm^{-3}, respectively). An earlier study by *Sax and Hudson* [1981] presented ground measurements of CCN in south central Florida and airborne measurements from east-west transects of the southern Florida peninsula. For the airborne measurements (S = 0.75%), concentrations peaked at 2500 cm^{-3} over the east coast, but dropped to between 250 and 500 cm^{-3} over the center of the peninsula. Ground measurements from the following year supported these data and demonstrated that the local concentrations in the boundary layer were dependent on wind speed and direction. Such a result is intuitive, given the nature of the Florida peninsula: large population centers along both coasts surround a rural interior. Off the eastern coast is the open Atlantic Ocean, where maritime conditions are the norm, while off the western coast lies the Gulf of Mexico, where there is often more recent continental influence.

[25] The range of CCN concentrations observed during the CRYSTAL-FACE campaign is in general agreement with these earlier studies. During CRYSTAL-FACE, data were collected both over land and the Gulf of Mexico near the southwestern coast of Florida (Figure 1). For this description of the general trends in CCN concentrations and the closure analysis that follows, the data from both CCN counters were averaged over 103 s to match the timescale of the individual size distributions from the DMA. Only data from level legs were included in the analysis. In this presentation, in-cloud data are included; cloud passes were brief relative to the averaging time, and it will be demonstrated in a later section that removing in-cloud data has a negligible impact on the results. As mentioned previously, the 0.85% S counter required periodic resaturation and was out of service ~5% of the time. The 0.2% S counter experienced temperature and pressure stability problems throughout the campaign that required some data filtering; these problems were usually seen at high altitudes and during changes in altitude.

[26] Table 3 summarizes the data from the Caltech CCN counter during the CRYSTAL-FACE campaign. For this instrument, operating at S = 0.85%, there are 868 measurements collected during 17 flights. Figure 8 shows a histogram of these data. The concentrations ranged from a low of 70 cm^{-3} (during CF-5) up to 5999 cm^{-3} (during CF-18); the average over the entire duration of the campaign was 533 cm^{-3}. However, Figure 8 indicates that the mean is skewed by a small number of data points at the upper end of the range; the vast majority of measured concentrations were below 1000 cm^{-3}, and the peak in the histogram lies between 250 and 300 cm^{-3}; the median is at 371 cm^{-3}. Almost all of the very high concentration measurements (>2000 cm^{-3}) are from CF-18 on 28 July. The final line on Table 3 indicates that if the data from CF-18 are omitted, the mean falls to 447 cm^{-3} and the upper boundary of the remaining data is 2332 cm^{-3}.

[27] The summary data for the Scripps CCN instrument, operating at S = 0.2%, are presented in Table 4. Over 12 flights, there were 353 sampling intervals, with measured concentrations ranging from 33 cm^{-3} (during CF-15) to 1553 cm^{-3} (during CF-10). The mean of these measurements is 306 cm^{-3}, but the histogram in Figure 9 shows that, as is the case for the higher supersaturation measurements, the mean is skewed by a proportionally small

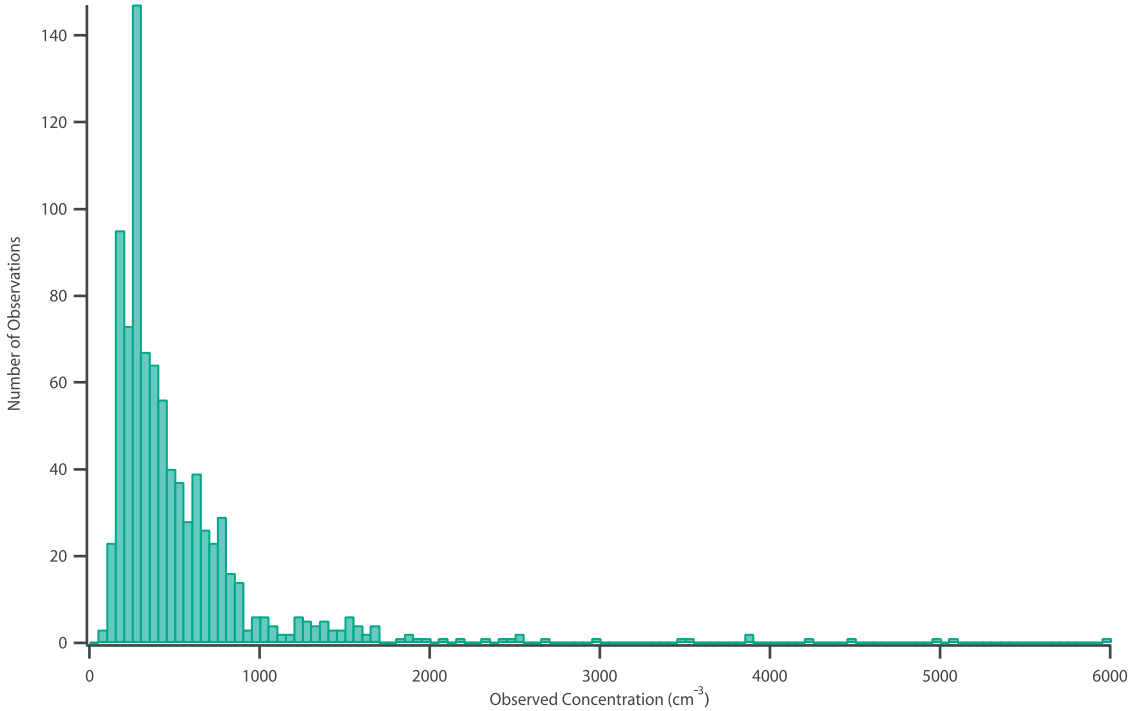

Figure 8. Histogram of CCN observations at $S = 0.85\%$.

number of high-concentration measurements. The median concentration is 233 cm^{-3}, and the peak in the histogram lies between 50 and 150 cm^{-3}.

[28] The histogram data at both supersaturations indicate that the air sampled during the campaign was typically marine and modified marine in character; air masses with more distinct continental and anthropogenic influence were encountered, but infrequently. At both $S = 0.2\%$ and $S = 0.85\%$, the peak in the histogram is below the mean reported by *Hudson and Yum* [2001] for marine aerosol, and the median concentrations from CRYSTAL-FACE are only slightly larger. The data ranges in Tables 3 and 4 may lead to the conclusion that the continental samples were spread over numerous flights; only during CF-10 was the continental influence obvious throughout the flight.

[29] The flight path of the Twin Otter during a CRYSTAL-FACE mission usually involved multiple altitudes with different patterns on each flight; much of the intraflight variability indicated in Tables 3 and 4 is a result of these complex flight patterns. Figures 10 and 11 show the relationship between CCN concentration and altitude. For clarity, the data from CF-18 are omitted from Figure 11 and from the present discussion; the very high concentrations at $S = 0.85\%$ during that flight all occurred at altitudes

Table 3. CCN Data Summary at $S = 0.85\%$[a]

Flight Number	Date	Number of Observations	Measured Concentration, cm^{-3}		Coefficient of Variation	
			Range	Mean	Range	Mean
CF-1	3 July	45	324–1040	660	0.03–0.20	0.07
CF-2	3 July	57	288–801	514	0.03–0.99	0.09
CF-3	6 July	44	155–872	606	0.03–0.19	0.07
CF-4	7 July	29	399–935	554	0.03–0.41	0.22
CF-5	7 July	93	70–391	185	0.04–1.44	0.20
CF-6	10 July	14	427–851	614	0.04–0.23	0.08
CF-10	18 July	18	1138–2332	1413	0.03–0.19	0.07
CF-11	18 July	34	407–1661	1052	0.03–0.31	0.09
CF-12	19 July	20	287–640	456	0.04–0.20	0.08
CF-13	19 July	96	195–515	313	0.04–0.67	0.13
CF-14	21 July	52	225–1105	615	0.03–0.32	0.09
CF-15	23 July	84	218–720	326	0.04–1.28	0.13
CF-16	25 July	60	199–774	305	0.04–0.38	0.10
CF-17	26 July	27	261–402	314	0.03–0.53	0.09
CF-18	28 July	89	286–5999	1283	0.03–0.90	0.22
CF-19	29 July	38	84–436	215	0.04–0.50	0.16
CF-20	29 July	68	151–1193	385	0.05–0.56	0.15
Overall		868	70–5999	533	0.03–1.44	0.13
Omitting CF-18		779	70–2332	447	0.03–1.44	0.12

[a]Each observation is averaged over 103 s. The coefficient of variation is the ratio of the standard deviation of each observation to the observed concentration.

Table 4. CCN Data Summary at $S = 0.2\%$[a]

Flight Number	Date	Number of Observations	Measured Concentration, cm^{-3}		Coefficient of Variation	
			Range	Mean	Range	Mean
CF-08	13 July	9	269–702	501	0.12–0.25	0.17
CF-09	16 July	36	129–582	391	0.07–0.27	0.13
CF-10	18 July	18	679–1553	850	0.10–0.49	0.22
CF-11	18 July	26	106–1310	649	0.10–0.76	0.36
CF-12	19 July	18	120–347	225	0.12–0.31	0.18
CF-13	19 July	25	39–80	55	0.25–0.76	0.46
CF-14	21 July	7	281–641	475	0.13–0.33	0.20
CF-15	23 July	55	33–304	141	0.12–0.68	0.28
CF-17	26 July	15	163–263	211	0.10–0.23	0.15
CF-18	28 July	52	219–1275	447	0.10–0.82	0.24
CF-19	29 July	28	50–261	109	0.13–0.43	0.25
CF-20	29 July	64	94–462	175	0.12–0.44	0.21
Overall		353	33–1553	306	0.07–0.82	0.24

[a]Each observation is averaged over 103 s. The coefficient of variation is the ratio of the standard deviation of each observation to the observed concentration.

between 700 and 1500 m. The outstanding feature in both figures is the group of high-concentration observations at about 1600 m. Although concentrations sufficiently high to be considered continental were seen on several flights, only during CF-10 and CF-11, the two flights on 18 July, was an air mass of apparent continental origin sampled for an extended time period. The lower concentrations also observed during CF-11 were from another flight leg at a higher altitude; the variation of concentration with altitude is much stronger than during other flights. The difference is explained by examining the back trajectory of the air mass for that day, using the National Oceanic and Atmospheric Administration's (NOAA) Hybrid Single-Particle Lagrangian Integrated Trajectory (HYSPLIT) model (available at http://www.arl.noaa.gov/ready/hysplit4.html, NOAA Air Resources Laboratory, Silver Spring, Maryland). For most of the mission, the air mass sampled by the Twin Otter had been aloft and/or over water for several days prior to being sampled. Figure 12 indicates a different history for 18 July: the air had been over the land for several days and the air at 1600 m had been at ground level 48 hours before. This air mass history explains the elevated concentrations seen on that day. For the rest of the data set, there appears to be some altitudinal dependence in CCN concentrations, but the temporal and local spatial variation appears to be more important.

6. Comparison of CCN Data With Aerosol-Size Distributions

[30] The importance of aerosol/CCN closure, and the difficulty in achieving it, is the primary motivation for this

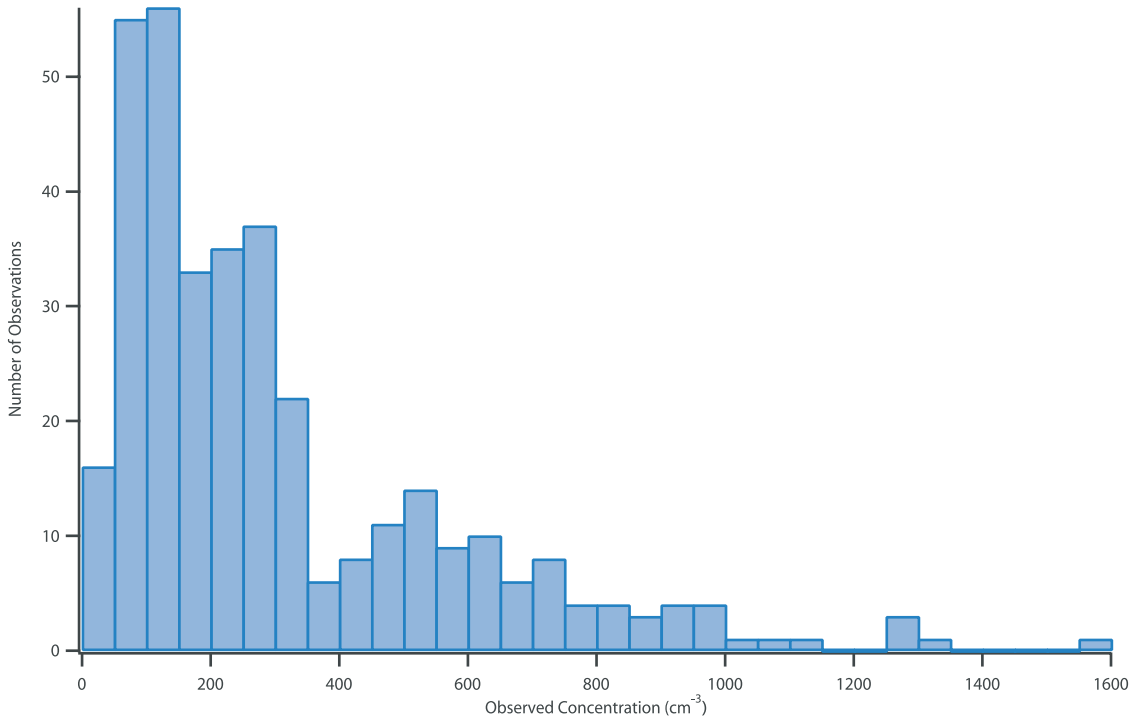

Figure 9. Histogram of CCN observations at $S = 0.2\%$.

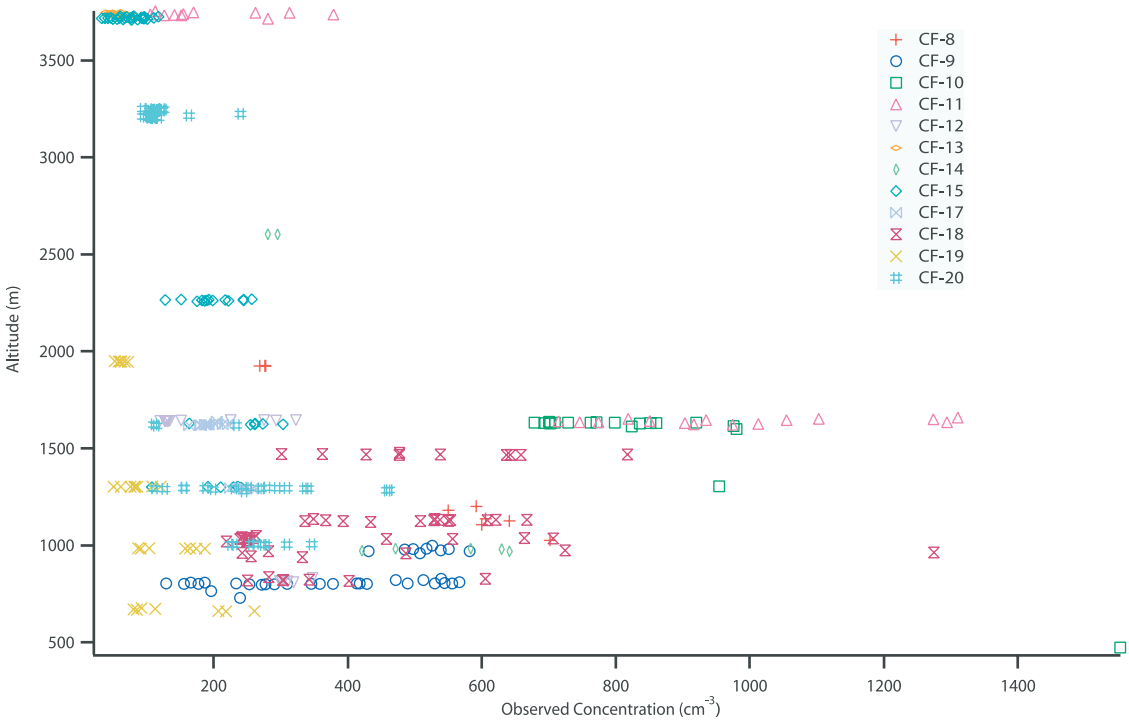

Figure 10. Altitude versus observed CCN concentration at $S = 0.2\%$.

work. The activation properties of the atmospheric aerosol determine in large part the extent of cloud formation and propagation, but our understanding of the processes involved is incomplete. Comparing measurements of CCN concentrations to predictions based on activation theory serves to validate both the measurement and the theory. During the CRYSTAL-FACE campaign, the DMA measured aerosol number size distributions, with an operating range of 10–900 nm. The scans from this DMA system last 103 s, and the instrument sampled from the same inlet as the CPC and CCN instruments; the data from both CCN counters were averaged to match the sampling interval of

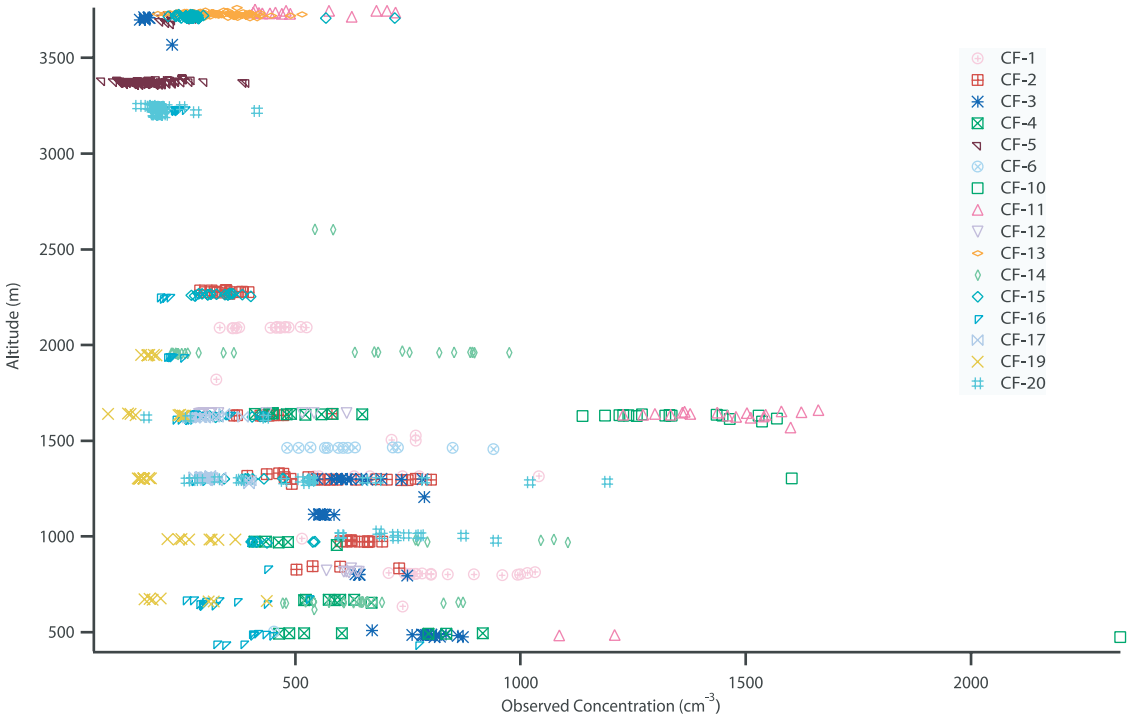

Figure 11. Altitude versus observed CCN concentration at $S = 0.85\%$. The observations from CF-18 are omitted for clarity.

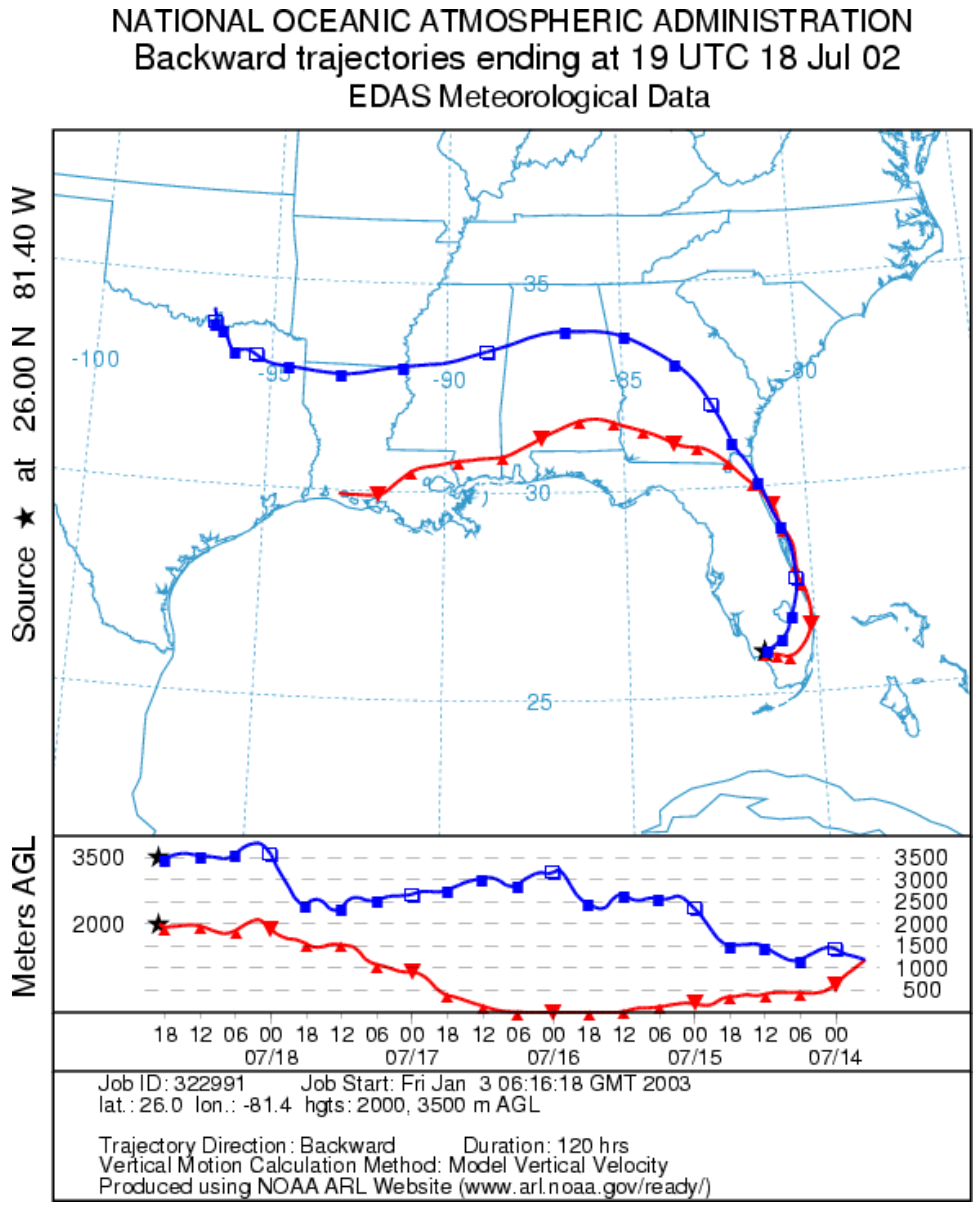

Figure 12. Simulated 120-hour back trajectories for the air mass sampled during flights CF-10 and CF-11. The plot is a product of the NOAA Air Resources Laboratory HYSPLIT model.

these size distributions. The operating range of the DMA includes the vast majority of the particles in the atmosphere, thus the CCN population can be effectively assumed to be a subset of the measured size distribution.

[31] For this analysis, the entire aerosol population was assumed to be pure ammonium sulfate. This is clearly a simplification, but it can be considered an obvious first step in estimating CCN concentrations from aerosol-size distributions, and the same assumption has been used in similar analyses previously [e.g., *Bigg*, 1986; *Martin et al.*, 1994; *Snider and Brenguier*, 2000]. Furthermore, the choice is supported, in general, by unpublished data obtained during CRYSTAL-FACE using the aerosol mass spectrometer (AMS) (R. Bahreini, personal communication, 2003). The assumed composition leads directly to a predicted cut size corresponding to the effective supersaturation in each CCN counter, calculated using Köhler theory where the van't Hoff factor for ammonium sulfate is held constant at three [cf. *Seinfeld and Pandis*, 1998]. For the counter operating at $S = 0.2\%$, this calculated cut size was 79 nm; for the Caltech instrument, which operated at $S = 0.85\%$, the cut size was 32 nm. The predicted CCN concentration is calculated by integrating upward from the cut size to the upper boundary of the size distribution.

[32] The long sampling time of the DMA system relative to other aerosol instruments limits its resolution during airborne measurements. During CRYSTAL-FACE, the nominal airspeed of the Twin Otter was 50 m s^{-1}; thus the spatial resolution of the DMA was approximately 5 km. The concentration at a given size is only measured at one point during each scan, and the data analysis implicitly assumes that the aerosol-size distribution is uniform over this spatial scale. In reality, the aerosol population frequently varies on scales shorter than 5 km. For this reason, it is not

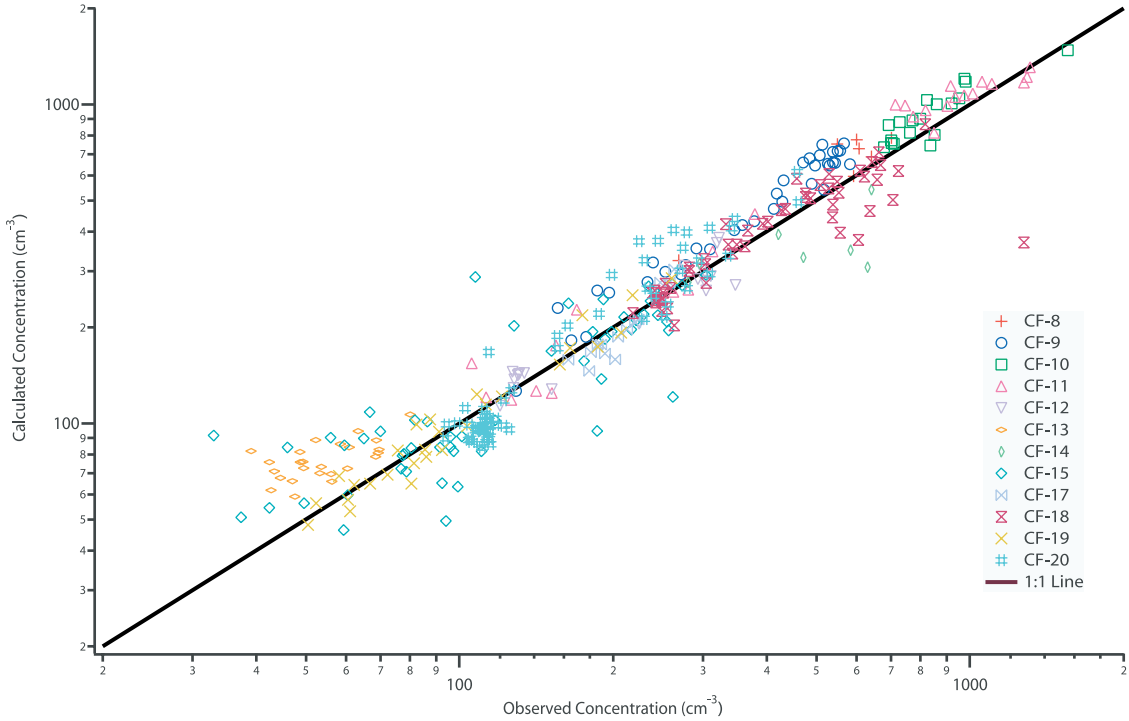

Figure 13. Scatterplot of the simplified closure analysis at $S = 0.2\%$.

necessarily expected that any individual comparison in the simplified closure analysis would indicate good agreement, but the uncertainties would presumably average to zero over the course of many measurements.

[33] The results of this simplified closure analysis are shown in scatterplot form in Figures 13 and 14. At $S = 0.2\%$, the agreement is excellent throughout the entire data set. A linear regression of predicted versus observed concentrations produces a slope of 1.026 and an intercept of 11.1 cm^{-3}, with an R^2 value of 0.912. If the intercept is forced to zero, the slope increases only slightly, to 1.047 ($R^2 = 0.911$). The overall correlation at $S = 0.85\%$ indicates some moderate overprediction: a slope of 1.264, with an intercept of -70.5 cm^{-3} ($R^2 = 0.840$); forcing a zero intercept reduces the slope to 1.201 ($R^2 = 0.835$). However, as was noted earlier, during portions of CF-18, both the CN and CCN (at $S = 0.85\%$) concentrations were much higher than were seen at any other point during the campaign. Omitting this flight from the regression reduces the slope to 1.093, with an intercept of -5.2 cm^{-3} ($R^2 = 0.770$); with a forced zero intercept, the slope is 1.085 ($R^2 = 0.770$).

[34] On the basis of these linear regressions, the overprediction of CCN at $S = 0.2\%$ is on average only 5% when assuming the idealized composition. At $S = 0.85\%$, the predicted concentration is 9% greater than the observation when omitting CF-18. These overestimates are very small, compared to the earlier studies discussed in section 2, and are within estimated measurement uncertainties (note that in the verification study for the Caltech instrument, Figure 4, the counting efficiency appears to be near 90%). Obviously, the compositional assumption is not strictly correct. The present analysis is as much a test of the assumption as of anything else, and the results support its use in cases like this one. The sensitivity of the results to the compositional assumption is examined further in the next section. In summary, the overpredictions are small, and the analysis validates the CCN measurements and the theory upon which the predicted concentrations are based.

7. Discussion

[35] The CCN population over southwest Florida and the surrounding waters during CRYSTAL-FACE is primarily marine in character and can be accurately calculated using the aerosol-size distribution. However, some assumptions used in the analysis can be scrutinized, particularly the inclusion of in-cloud data in the analysis and the assumption of a pure ammonium sulfate aerosol. Also, at several points in the analysis, the CCN observations at $S = 0.85\%$ from CF-18 have been omitted. The reasoning behind these decisions and the impact they have on the analysis are discussed below.

7.1. In-Cloud Sampling

[36] The decision to include in-cloud observations in the analysis was primarily one of convenience. Cloud passes were usually very brief, and it was assumed that the impact of including these data would be negligible. To confirm this, the CCN data at $S = 0.85\%$ were filtered to remove data collected in-cloud, and the results were compared to the unfiltered data. The filter removed observations where the average liquid water content (over the 103-s sampling period), as measured by a Forward Scattering Spectrometer Probe (FSSP, from PMS, Inc.), was greater than 500 μg cm^{-3}. This effectively removed all data points wherein a portion of the sample time was in-cloud, 17% of the data set. The average CCN concentration of the filtered data set is 518 cm^{-3}, a decrease of 3%. The effect on the closure analysis was

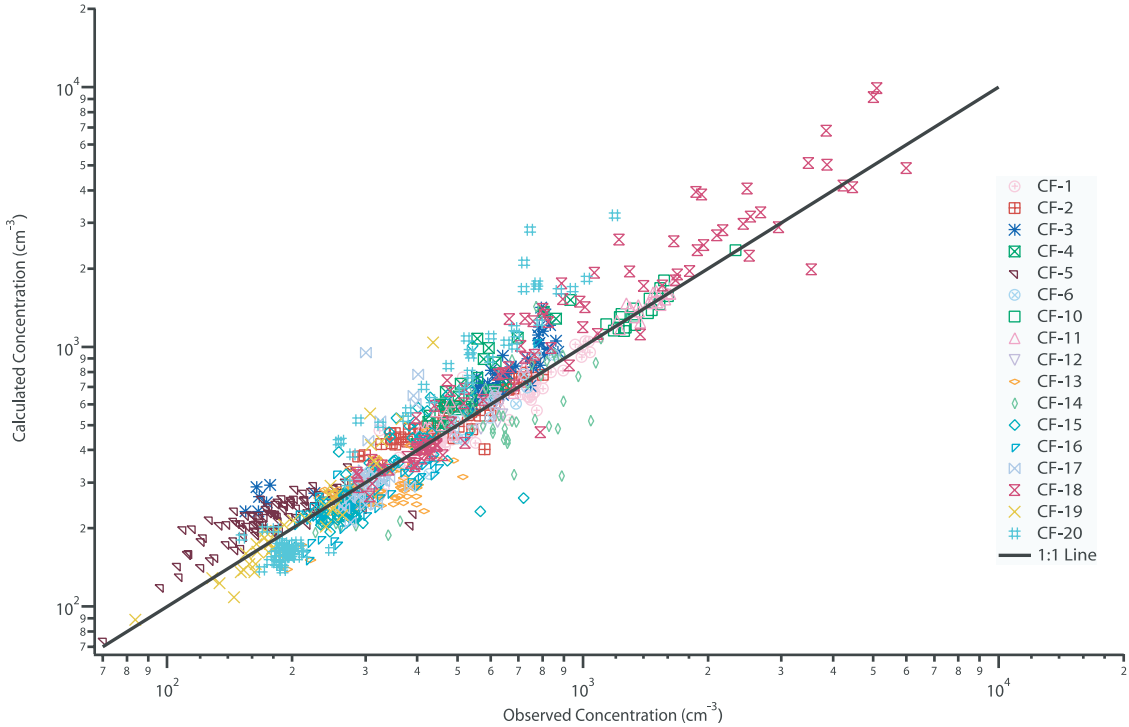

Figure 14. Scatterplot of the simplified closure analysis at $S = 0.85\%$.

even smaller: after removing the in-cloud samples, the slope of the curve fit (predicted versus observed concentration) increases to 1.240 (R^2 = 0.826, intercept forced to zero), a 1% difference. This confirms that the inclusion of in-cloud samples has a negligible impact on the overall analysis.

7.2. Aerosol Composition

[37] For the simplified closure analysis in section 6, the aerosol was assumed to be composed entirely of ammonium sulfate. The results indicate that this was a viable procedure in this case, even though the assumption could not have been strictly true. Each of the successful closure analyses discussed in section 2 relied on more detailed compositional assumptions, as did nearly all of the studies where closure was not achieved. Incomplete understanding of the role of composition in establishing the aerosol/CCN relationship was cited in many cases as a primary reason why the closure analysis was unsuccessful.

[38] One reason the idealized ammonium sulfate compositional assumption works so well here may lie in the mixing state of the aerosol. The viability of the assumption provides strong evidence of an internally mixed aerosol. Substantial external mixing of the population would mean that some fraction of the aerosol would have little or no ammonium sulfate. Whatever their actual composition, these particles (at equivalent diameters) would almost certainly activate at higher critical supersaturations; sodium chloride is the only common atmospheric species that activates more readily than ammonium sulfate, and *Twomey* [1971] determined that most atmospheric CCN are not NaCl. Explaining the results in section 6 using an externally mixed aerosol requires that the concentration of smaller NaCl particles that activate at 0.85% (or 0.2%) supersaturation be consistently offset by an equivalent number of larger, less readily activated particles; this result is highly unlikely.

[39] However, if the aerosol is internally mixed, it is expected that the population, as a whole, would be relatively insensitive to the presence of insoluble species. *Roberts et al.* [2002] demonstrated using a prescribed size distribution that replacing half of the soluble mass (in this case, ammonium bisulfate) with insoluble organic material throughout the entire aerosol population reduced the activated fraction by only about 10% (at $S = 0.85\%$). The effect is somewhat more pronounced at lower supersaturations; the same replacement of soluble mass with insoluble mass leads to a drop in activated fraction on the order of 35% at $S = 0.2\%$. This result is not surprising; although the replacement of soluble mass with insoluble mass can have a large effect on activation properties for particles whose critical supersaturations are near the effective supersaturation of the instrument, the integral nature of the measurement means that the overall impact will be substantially less important. In practical terms, substituting insoluble mass for soluble mass would cause the activation cut size to shift by some undetermined number of channels. This relative insensitivity to the presence of insoluble compounds lends credence to the idealized ammonium sulfate composition used in this analysis.

[40] The selection of ammonium sulfate as opposed to other species also impacts the analysis. The choice reflects the predominance of ammonium and sulfate in the atmospheric aerosol particles smaller than 1 μm, as a result of cloud processing [*Seinfeld and Pandis*, 1998]. However, the composition of the resultant particle is influenced by the relative abundance of ammonia and sulfur dioxide at the time of processing. Ammonium sulfate production

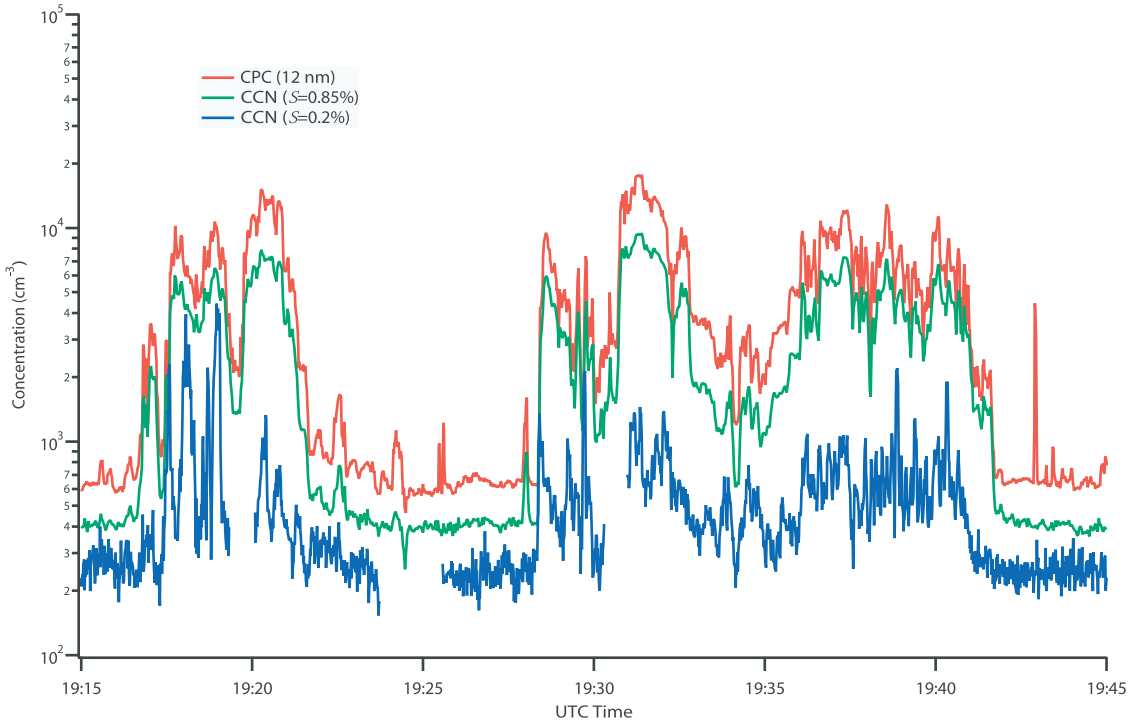

Figure 15. Time series for a portion of flight CF-18. Note how the aerosol concentrations measured by the CPC change rapidly by more than an order of magnitude. The high concentrations were atypical of the conditions normally encountered during CRYSTAL-FACE.

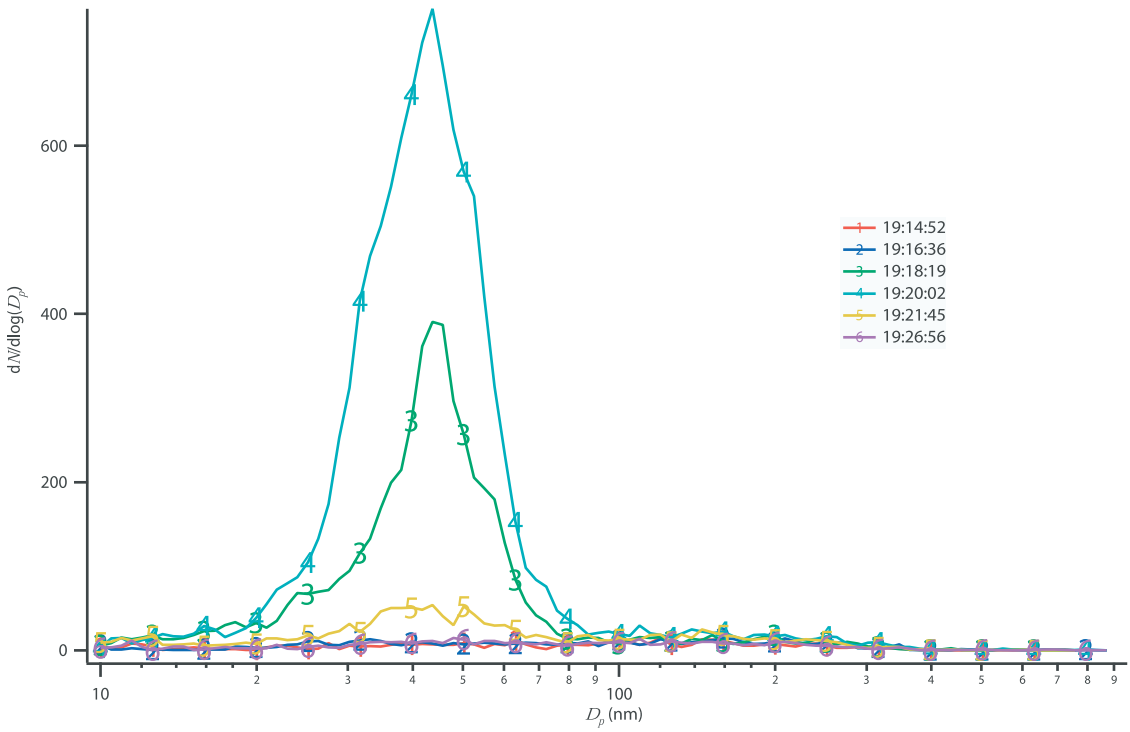

Figure 16. Consecutive size distributions from the DMA for the first half of the time series in Figure 15. The large peak that dominates the spectrum at 1920:02 UT disappears almost completely in the next scan. Nearly all of the particles in the scans showing elevated concentrations are below the size at which ammonium sulfate particles would activate at S = 0.2% (i.e., 80 nm).

dominates at high ammonia concentrations; at lower ammonia concentrations, ammonium bisulfate is the more common product. To determine the sensitivity of the closure analysis to the particular species chosen as the solute, the statistics were recalculated using a different composition, ammonium bisulfate. In practical terms, this means increasing the cut size from 79 to 87 nm for the comparison at S = 0.2% and from 32 to 35 nm for the analysis at S = 0.85%. At S = 0.2%, the adjustment resulted in a decrease in the slope of the fitted line from 1.047 to 0.939; the R^2 is nearly unchanged (0.911 and 0.909, respectively). At S = 0.85%, the reanalysis results in the slope of the fitted line dropping from 1.234 (R^2 = 0.822) to 1.201 (R^2 = 0.835). If the data from flight CF-18 are omitted, the slope drops to 1.085 (R^2 = 0.770). Thus if the aerosol is assumed to be ammonium bisulfate rather than ammonium sulfate, the size distribution underpredicts the CCN concentration somewhat at S = 0.2% and overpredicts the CCN concentration somewhat at 0.85%. This confirms that the success of the analysis is not entirely dependent on the precise soluble species used to define the aerosol composition.

7.3. Flight CF-18

[41] During the 28 July flight, CF-18, several instruments on the CIRPAS Twin Otter measured particle concentrations far greater than at any other time during the CRYSTAL-FACE campaign. The source or sources of these particles is not immediately clear, but the result was that aerosol (and CCN) concentrations rapidly changed by more than an order of magnitude, as can be seen in Figure 15. The CCN concentration at S = 0.85% tracks closely with the total aerosol concentration, while CCN at S = 0.2% appear to correlate less well; this is an indication that the particles were too small to be activated at the lower supersaturation. The size distribution data corroborate this (Figure 16); the vast majority of particles are smaller than 80 nm, the nominal cut size at which ammonium sulfate particles activate when S = 0.2%. This explains why the concentrations at the lower supersaturation are not atypically high. Figure 16 also provides some explanation as to why the closure analysis from CF-18 involved large underpredictions as well as overpredictions. The consecutive size distributions show how rapid the transitions were between elevated and normal particle concentrations. As was discussed in the previous section, the scan time for the DMA was sufficiently long that it could miss these particles: if the transition occurs while the DMA is scanning at the upper end of the size range, the huge numbers of small particles would not be observed. This is true at all times, but usually the atmospheric particle concentrations are spatially stable enough that the scan rate is not an issue; that does not appear to be the case here. The extremely high concentrations and large spatial variation for the small particles on this flight are very interesting and worthy of further study. However, the atypical concentrations on this day justify omitting them from the closure analysis and from the description of the CCN trends for the region.

8. Conclusions

[42] Information gathered from the CIRPAS Twin Otter during the July 2002 CRYSTAL-FACE campaign provides a clear picture of the character of the atmospheric aerosol along the coast of southwest Florida. Included in the Twin Otter payload were two cloud condensation nucleus counters that employed a recently developed technique for maintaining a stable constant supersaturation in order to make continuous real-time measurements of CCN. These instruments, operating at supersaturations of 0.2 and 0.85%, were well characterized in the laboratory and in the field, and their performance was consistent with those of other aerosol counters on board the aircraft.

[43] The CCN concentrations measured over the course of the campaign by the two instruments were in general agreement with those from earlier studies in the region. At S = 0.2%, the mean concentration over the course of the campaign was 306 cm^{-3}, while the median was 233 cm^{-3}. At S = 0.85%, the mean and median were 533 and 371 cm^{-3}, respectively. These data indicate that the majority of observations are best described as marine in character. Of the 19 flights for which data are available, only two air masses were sampled that had a distinct continental influence.

[44] The extensive data set from the CRYSTAL-FACE campaign was used as the basis for a simplified closure analysis to determine whether the CCN concentration could be accurately predicted by assigning an assumed composition to a measured aerosol-size distribution. The analysis proved successful: at S = 0.2% the calculated concentration was on average 3% greater than the prediction, with an R^2 value of 0.91. At S = 0.85%, the overall ratio of calculated to measured concentrations was 1.09 (R^2 = 0.77), when the atypical data from CF-18 are excluded. The analysis indicates that for conditions like those encountered during the CRYSTAL-FACE campaign it may be possible to accurately calculate the concentrations of CCN over a range of supersaturations from the aerosol-size distribution by assuming a pure ammonium sulfate composition.

[45] More study is required in order to determine whether it is a generally applicable practice to predict CCN concentrations from the aerosol-size distribution using an idealized composition. There are certainly conditions, like the elevated concentrations encountered during CF-18, where assuming a pure composition is not sufficient for characterizing the CCN population. The measurements made during the CRYSTAL-FACE campaign establish new instrumentation for accurate in situ CCN measurements for use in future campaigns.

[46] **Acknowledgments.** The authors acknowledge Athanasios Nenes for assistance with simulating the performance of the CCN instruments. This work was supported by National Aeronautics and Space Administration grant NAG5-11549 and the Office of Naval Research.

References

Albrecht, B., Aerosols, cloud microphysics and fractional cloudiness, *Science*, *245*, 1227–1230, 1989.

Bigg, E. K., Discrepancy between observation and prediction of concentrations of cloud condensation nuclei, *Atmos. Res.*, *20*, 82–86, 1986.

Cantrell, W., G. Shaw, C. Leck, L. Granat, and H. Cachier, Relationships between cloud condensation nuclei spectra and aerosol particles on a south-north transect of the Indian Ocean, *J. Geophys. Res.*, *105*, 15,313–15,320, 2000.

Cantrell, W., G. Shaw, G. R. Cass, Z. Chowdhury, L. S. Hughes, K. A. Prather, S. A. Guazzotti, and K. R. Coffee, Closure between aerosol particles and cloud condensation nuclei at Kaashidhoo Climate Observatory, *J. Geophys. Res.*, *106*, 28,711–28,718, 2001.

Charlson, R. J., J. H. Seinfeld, A. Nenes, M. Kulmala, A. Laaksonen, and M. C. Facchini, Reshaping the theory of cloud formation, *Science*, *292*, 2025–2026, 2001.

Chuang, P. Y., D. R. Collins, H. Pawlowska, J. R. Snider, H. H. Jonsson, J.-L. Brenguier, R. C. Flagan, and J. H. Seinfeld, CCN measurements during ACE-2 and their relationship to cloud microphysical properties, *Tellus, Ser. B*, *52*, 843–867, 2000a.

Chuang, P. Y., A. Nenes, J. N. Smith, R. C. Flagan, and J. H. Seinfeld, Design of a CCN instrument for airborne measurement, *J. Atmos. Oceanic Technol.*, *17*, 1005–1019, 2000b.

Covert, D. S., J. L. Gras, A. Wiedensohler, and F. Stratmann, Comparison of directly measured CCN with CCN modeled from the number-size distribution in the marine boundary layer during ACE 1 at Cape Grim, Tasmania, *J. Geophys. Res.*, *103*, 16,597–16,608, 1998.

Cruz, C. N., and S. N. Pandis, The effect of organic coatings on the cloud condensation nuclei activation of inorganic atmospheric aerosol, *J. Geophys. Res.*, *103*, 13,111–13,123, 1998.

Durkee, P. A., et al., The impact of ship-produced aerosols on the microstructure and albedo of warm marine stratocumulus clouds: A test of MAST hypotheses 1i and 1ii, *J. Atmos. Sci.*, *57*, 2554–2569, 2000.

Garrett, T. J., L. F. Radke, and P. V. Hobbs, Aerosol effects on cloud emissivity and surface longwave hearing in the arctic, *J. Atmos. Sci.*, *59*, 769–778, 2002.

Hegg, D. A., L. F. Radke, and P. V. Hobbs, Measurements of Aitken nuclei and cloud condensation nuclei in the marine atmosphere and their relation to the DMS-cloud-climate hypothesis, *J. Geophys. Res.*, *96*, 18,727–18,733, 1991.

Hegg, D. A., R. J. Ferek, and P. V. Hobbs, Cloud condensation nuclei over the Arctic Ocean in early spring, *J. Appl. Meteorol.*, *34*, 2076–2082, 1995.

Hegg, D. A., S. Gao, W. Hoppel, G. Frick, P. Caffrey, W. R. Leaitch, N. Shantz, J. Ambrusko, and T. Albrechcinski, Laboratory studies of the efficiency of selected organic aerosols as CCN, *Atmos. Res.*, *58*, 155–166, 2001.

Hitzenberger, R., A. Berner, H. Giebl, R. Kromp, S. M. Larson, A. Rouc, A. Koch, S. Marischka, and H. Puxbaum, Contribution of carbonaceous material to cloud condensation nuclei concentrations in European background (Mt. Sonnblick) and urban (Vienna) aerosols, *Atmos. Environ.*, *33*, 2647–2659, 1999.

Hudson, J. G., Cloud condensation nuclei near marine cumulus, *J. Geophys. Res.*, *98*, 2693–2702, 1993.

Hudson, J. G., and P. R. Frisbie, Surface cloud condensation nuclei and condensation nuclei measurements at Reno, Nevada, *Atmos. Environ., Part A*, *25*, 2285–2299, 1991.

Hudson, J. G., and S. S. Yum, Maritime-continental drizzle contrasts in small cumuli, *J. Atmos. Sci.*, *58*, 915–926, 2001.

Intergovernmental Panel on Climate Change (IPCC), *Climate Change 2001: The Scientific Basis*, edited by J. T. Houghton et al., Cambridge Univ. Press, New York, 2001.

Ji, Q., G. E. Shaw, and W. Cantrell, A new instrument for measuring cloud condensation nuclei: Cloud condensation nucleus ''remover'', *J. Geophys. Res.*, *103*, 28,013–28,019, 1998.

Johnson, D. W., S. R. Osborne, and J. P. Taylor, The effects of a localized aerosol perturbation on the microphysics of a stratocumulus cloud layer, in *Nucleation and Atmospheric Aerosols 1996*, edited by M. Kulmala and P. E. Wagner, Elsevier Sci., New York, 1996.

Liu, P. S. K., W. R. Leaitch, C. M. Banic, S.-M. Li, D. Ngo, and W. J. Megaw, Aerosol observations at Chebogue Point during the 1993 North Atlantic Regional Experiment: Relationships among cloud condensation nuclei, size distribution, and chemistry, *J. Geophys. Res.*, *101*, 28,971–28,990, 1996.

Martin, G. M., D. W. Johnson, and A. Spice, The measurement and parameterization of effective radius of droplets in warm stratocumulus clouds, *J. Atmos. Sci.*, *51*, 1823–1842, 1994.

Nenes, A., P. Y. Chuang, R. C. Flagan, and J. H. Seinfeld, A theoretical analysis of cloud condensation nucleus (CCN) instruments, *J. Geophys. Res.*, *106*, 3449–3474, 2001.

Nenes, A., R. J. Charlson, M. C. Facchini, M. Kulmala, A. Laaksonen, and J. H. Seinfeld, Can chemical effects on cloud droplet number rival the first indirect effect?, *Geophys. Res. Lett.*, *29*(17), 1848, doi:10.1029/2002GL015295, 2002.

Ramanathan, V., R. D. Cess, E. F. Harrison, P. Minnis, B. R. Barkstrom, E. Ahmad, and D. Hartmann, Cloud-radiative forcing and climate: Results from the Earth Radiation Budget Experiment, *Science*, *243*, 57–63, 1989.

Raymond, T. M., and S. N. Pandis, Cloud activation of single-component organic aerosol particles, *J. Geophys. Res.*, *107*(D24), 4787, doi:10.1029/2002JD002159, 2002.

Roberts, G. C., P. Artaxo, J. Zhou, E. Swietlicki, and M. O. Andreae, Sensitivity of CCN spectra on chemical and physical properties of aerosol: A case study from the Amazon Basin, *J. Geophys. Res.*, *107*(D20), 8070, doi:10.1029/2001JD00583, 2002.

Rogers, C. F., and P. Squires, A new device for studies of cloud condensation nuclei active at low supersaturations, in *Atmospheric Aerosols and Nuclei*: *Proceedings of the Ninth International Conference on Atmospheric Aerosols, Condensation, and Ice Nuclei Held at University College, Galway, Ireland, 21–27 September, 1977*, edited by A. F. Roddy and T. C. O'Connor, Galway Univ. Press, Ireland, 1981.

Rosenfeld, D., TRMM observed first direct evidence of smoke from forest fires inhibiting rainfall, *Geophys. Res. Lett.*, *26*, 3105–3108, 1999.

Rosenfeld, D., Suppression of rain and snow by urban and industrial air pollution, *Science*, *287*, 1793–1796, 2000.

Sax, R. I., and J. G. Hudson, Continentality of the south Florida summertime CCN aerosol, *J. Atmos. Sci.*, *38*, 1467–1479, 1981.

Seinfeld, J. H., and S. N. Pandis, *Atmospheric Chemistry and Physics*: *From Air Pollution to Climate Change*, 1326 pp., John Wiley, Hoboken, N. J., 1998.

Snider, J. R., and J.-L. Brenguier, Cloud condensation nuclei and cloud droplet measurements during ACE-2, *Tellus, Ser. B*, *52*, 828–842, 2000.

Twomey, S., The composition of cloud nuclei, *J. Atmos. Sci.*, *28*, 377–381, 1971.

Twomey, S., Influence of pollution on the short-wave albedo of clouds, *J. Atmos. Sci.*, *34*, 1149–1152, 1977.

Wang, J., R. C. Flagan, and J. H. Seinfeld, A differential mobility analyzer (DMA) system for submicron aerosol measurements at ambient relative humidity, *Aerosol Sci. Technol.*, *37*, 46–52, 2003.

Wood, R., et al., Boundary layer and aerosol evolution during the 3rd Lagrangian experiment of ACE-2, *Tellus, Ser. B*, *52*, 401–422, 2000.

Zhou, J., E. Swietlicki, O. H. Berg, P. P. Aalto, K. Hämeri, E. D. Nilsson, and C. Leck, Hygroscopic properties of aerosol particles over the central Arctic Ocean during summer, *J. Geophys. Res.*, *106*, 32,111–32,123, 2001.

R. C. Flagan, T. A. Rissman, J. H. Seinfeld, T. M. VanReken, and V. Varutbangkul, Department of Chemical Engineering, California Institute of Technology, Mail Code 210-41, 1200 East California Boulevard, Pasadena, CA 91125, USA. (flagan@caltech.edu; rissman@its.caltech.edu; seinfeld@caltech.edu; vanreken@its.caltech.edu; tomtor@its.caltech.edu)

H. H. Jonsson, Center for Interdisciplinary Remotely Piloted Aircraft Studies, United States Naval Postgraduate School, 3240 Imjin Road, range #510, Marina, CA 93633, USA. (hjonsson@nps.navy.mil)

G. C. Roberts, Center for Atmospheric Sciences, Scripps Institution of Oceanography, 9500 Gilman Drive #0239, San Diego, CA 92093, USA. (greg@fiji.ucsd.edu)